Nucleon — nucleus diffraction scattering and nuclear structure

A. G. Sitenko

Institute of Theoretical Physics, Academy of Sciences, Ukrainian SSR
Fiz. El. Chast. Atom. Yad., 4, 546-584 (1973)

This paper is devoted to a consideration of elastic and inelastic nucleon—nucleus scattering at high energy in the diffraction approximation. For particle scattering in a central field, a solution of the Lippman—Schwinger equation in the high-energy approximation is discussed. On the basis of the resultant solution, a generalized Huygens principle describing nuclear diffraction processes is formulated. Scattering of a fast particle by a system of bound particles is discussed and the effects of multiple scattering are investigated. Nucleon scattering by the simplest nucleus — the deuteron — is considered in detail. The diffraction approximation is compared with various versions of the impulse approximation. Using elastic scattering of protons by the ^{12}C nucleus as an example, a quantitative estimate is made of the accuracy of the plane-wave impulse approximation and of the distorted-wave impulse approximation as compared to the diffraction approximation. The multipole formalism used for the description of nucleon—nucleus inelastic scattering in the case of small momentum transfer is considered in detail. A number of specific inelastic transitions induced in nuclei by high-energy protons are discussed. Various possibilities for extracting information about nuclear structure from nucleon—nucleus scattering data at high energies are discussed.

1. INTRODUCTION

The investigation of the scattering of fast particles by nuclei is a most important source of information about nuclear structure. Elastic and inelastic scattering is possible in the collision of fast particles with nuclei. The study of elastic scattering of fast particles makes it possible to obtain information about nuclear size, nucleon density distribution within the nucleus, and other characteristics of nuclei in the ground state. The study of inelastic scattering of fast particles by nuclei can be used to determine the quantum number of excited states of nuclei and to determine the nature of these states.

Electrons and nucleons are the most suitable particles for studying nuclear structure. In the case of electrons, scattering is determined by the electromagnetic interaction; from electron scattering data, one can therefore only determine the electromagnetic characteristics of the nucleus (charge radius, charge distribution in the nucleus, width of levels excited by electromagnetic interaction, and various electromagnetic form factors for ground and excited states).[1,2] Nuclear interactions appear in nucleon scattering; therefore, the scattering cross section is characterized by a significantly higher value than in the electron case. Here the scattering depends not only on the charge distribution in the nucleus, but also on the nucleon density distribution and the distribution of other nonelectromagnetic quantities. In addition, levels of a different nature (not excited through the electromagnetic interaction) may be excited in inelastic nucleon scattering and the phenomenon of charge exchange is also possible.

A considerable number of papers, both experimental and theoretical, have been devoted to study of interactions of fast nucleons with nuclei. The impulse approximation has been used for the description of elastic and inelastic nucleon—nucleus scattering in many papers.[3-11] The impulse approximation is applicable when the energy of the incident nucleon is considerably greater than the binding energy of individual nucleons in the nucleus. In the impulse approximation, the cross section for any nucleon—nucleus interaction is expressed in terms of the nucleon—nucleon scattering amplitude and some form factor which is associated with nuclear structure.[3] The form factors mentioned can be calculated on the basis of a given nuclear model. Direct comparison of data on inelastic nuclear scattering of nucleons and electrons for given transitions where the form factors appearing in the corresponding cross sections were identical was used[4,6] to verify the applicability of the impulse approximation. In refs. 5-11, a considerable number of calculations were made for various inelastic transitions in light nuclei and for a number of nuclear models. The impulse approximation was used, with distortion of the incoming and outgoing nucleon waves. Two-nucleon amplitudes were calculated from data for the interaction of two nucleons of the appropriate energies.

Investigations based on consideration of the diffraction nature of the nuclear interaction at high energies are more precise than those using the impulse approximation. Indeed, experimental data on nucleon—nucleon scattering indicate that the interaction at sufficiently high energies is of a diffraction nature. Diffraction phenomena occur when the wavelength of the relative motion of the colliding particles is small in comparison with the characteristic dimensions of the region in which the interaction occurs. In this case, the differential scattering cross section is characterized by a sharply defined maximum at small angles, the width of which is determined by the ratio between the wavelength and the dimensions of the interaction region. This type of scattering does not depend completely on the detailed nature of the interaction, which need only be characterized by a finite radius, and is a direct consequence of the wave nature of the colliding particles. Since nuclear dimensions are usually considerably greater than the radius of nucleon—nucleon interactions, nucleon—nucleus scattering at sufficiently high energies can be described by analogy with optical diffraction, i.e., can be considered as multiple diffraction scattering by individual nucleons.

The diffraction approach makes it possible to express the nucleon—nucleus and form factors which depend on nuclear structure. In contrast to the impulse approximation, the effects of multiple scattering are taken into account logically in the diffraction approach. Since interference plays an important role in multiple scattering, interaction processes are very sensitive to spatial structure in the nucleus. Diffraction theory for nuclear processes involving the participation of complex particles was developed independently in refs. 12 and 13, and is widely used at the present time for analysis of experimental data on nucleon scattering (and on the scattering of pions and other strongly interacting particles) by nuclei at high energies (see refs. 14-16).

In the consideration of transitions in nuclei associated with small momentum transfer for the scattered nucleon, it is convenient to use multipole expansion.[17] In this instance, the structural form factor appearing in the cross section for any process is directly expressed through the square of the modulus of the reduced matrix element for the corresponding multipole moment of the nucleus. Considering the charge degrees of freedom of the nucleons, a nucleus can be described by multipoles of sixteen types of multipolarity. Rigidly defined selection rules correspond to each transition of given multipolarity. Use of the multipole formalism facilitates the corresponding calculations and makes it possible to clarify the physical nature of the various transitions in nuclei. Initially, multipole analysis of the scattering of fast nucleons by nuclei used the impulse approximation;[10,11] subsequently, this method was generalized to take into account the effects of multiple scattering.[18]

This paper is devoted to consideration of elastic and inelastic nucleon–nucleus scattering at high energies in the diffraction approximation. First, a solution of the Lippman–Schwinger equation in the high-energy approximation is considered for particle scattering in a central field. On the basis of the resultant solution, a generalized Huygens principle describing nuclear diffraction processes is formulated. In the high-energy approximation, particle scattering by a system of bound particles is then considered and the effects of multiple scattering investigated. Scattering of nucleons by the simplest nucleus – the deuteron – is discussed in detail. The diffraction approximation is compared with various versions of the impulse approximation. Using elastic scattering of protons by the ^{12}C nucleus, quantitative estimates are made of the accuracy of the plane-wave and distorted-wave impulse approximations when compared with the diffraction approximation. The multipole formalism used for the description of nucleon–nucleus inelastic scattering in the case of small momentum transfer is discussed in detail. A number of specific inelastic nuclear transitions produced by high-energy protons are considered. Various possibilities for extracting information about nuclear structure from data on nucleon–nucleus scattering at high energies are discussed.

2. HIGH-ENERGY APPROXIMATION AND GENERALIZED HUYGENS PRINCIPLE

We consider the elastic collision of two particles, the interaction between which we shall describe by the potential $V(\mathbf{r})$. In the center-of-mass system, the two-particle scattering problem reduces to the problem of the scattering of a single particle in the field of a fixed force center $V(\mathbf{r})$. The wave function ψ describing the scattering is defined by the Lippman–Schwinger equation

$$\psi = \varphi + g_0 V \psi, \tag{2.1}$$

where φ is the unperturbed wave function (incident wave); g_0 is the Green's function

$$g_0 = (E - H_0 + io)^{-1} \tag{2.2}$$

($H_0 = \mathbf{p}^2/2\mu$ is the unperturbed Hamiltonian; E is the energy of the system, and μ is the reduced mass).

Choosing as the unperturbed wave function a plane wave corresponding to an incident particle with momentum $\mathbf{k}$:

$$\varphi_{\mathbf{k}}(\mathbf{r}) = e^{i\mathbf{k}\mathbf{r}} \tag{2.3}$$

(momentum $\mathbf{k}$ and energy E are connected by the relation $E = \mathbf{k}^2/2\mu$), Eq. (2.1) is conveniently rewritten in coordinate representation as

$$\psi_{\mathbf{k}}(\mathbf{r}) = e^{i\mathbf{k}\mathbf{r}} + \int d\mathbf{r}' g_0(\mathbf{r}, \mathbf{r}') V(\mathbf{r}') \psi_{\mathbf{k}}(\mathbf{r}'), \tag{2.4}$$

where

$$g_0(\mathbf{r}, \mathbf{r}') = -\frac{\mu}{2\pi} \cdot \frac{e^{ik|\mathbf{r}-\mathbf{r}'|}}{|\mathbf{r}-\mathbf{r}'|}. \tag{2.5}$$

Using the asymptote for the Green's function (2.5) when $r \to \infty$, it is easy to see from Eq. (2.4) that the wave function $\psi_{\mathbf{k}}(\mathbf{r})$ at large distances represents the superposition of plane and spherically diverging waves. The coefficient for the spherically diverging wave determines the scattering amplitude

$$f(\mathbf{k}, \mathbf{k}') = -\frac{\mu}{2\pi} \int d\mathbf{r} e^{-i\mathbf{k}'\mathbf{r}} V(\mathbf{r}) \psi_{\mathbf{k}}(\mathbf{r}), \tag{2.6}$$

where $\mathbf{k}'$ is the particle momentum after scattering.

If the energy of the incident particle is sufficiently high so that the wavelength $\lambda = k^{-1}$ is small in comparison with the characteristic dimensions r_0 of the region of interaction ($kr_0 \gg 1$), the scattering amplitude (2.6) is characterized by a sharply defined maximum at small scattering angles, i.e., for small angles between the vectors $\mathbf{k}$ and $\mathbf{k}'$. The presence of the indicated maximum in the scattering amplitude means that only small changes in momentum are important in the scattering of high-energy particles. Thus the so-called high-energy, or eikonal, approximation in which only intermediate states corresponding to momentum values close to the initial value are taken into account is quite applicable for the description of the scattering of such particles.

We represent the unperturbed Hamiltonian H_0 in the following form:

$$\begin{aligned} H_0 &\equiv \frac{1}{2\mu}(\mathbf{p}-\mathbf{k})(\mathbf{p}+\mathbf{k}) + \frac{\mathbf{k}^2}{2\mu} \\ &\equiv \frac{1}{\mu}(\mathbf{p}-\mathbf{k})\mathbf{k} + \frac{\mathbf{k}^2}{2\mu} + \frac{1}{2\mu}(\mathbf{p}-\mathbf{k})^2. \end{aligned} \tag{2.7}$$

The high-energy approximation involves neglect of the last term in Eq. (2.7), i.e., in replacement of the unperturbed Hamiltonian H_0 by the approximate eikonal Hamiltonian:[19]

$$\widetilde{H}_0 = \frac{1}{\mu}(\mathbf{p}-\mathbf{k})\mathbf{k} + \frac{\mathbf{k}^2}{2\mu}. \tag{2.8}$$

It is obvious that such a substitution is only valid for diffraction scattering where only small changes in momentum are important. The eikonal Hamiltonian (2.8) is nondiagonal in the energy representation; in the high-energy approximation, conservation of energy is replaced by conservation of the projection of the momentum on the direction of **k**:

$$\mathbf{pk} = \text{const.}$$

Replacement of the Hamiltonian H_0, which depends on the square of the momentum operator **p**, by the eikonal Hamiltonian $\widetilde{H}_0$, which is linear with respect to **p**, considerably simplifies the scattering problem. Dependence of the eikonal Hamiltonian $\widetilde{H}_0$ only on the momentum component along the direction of the initial momentum **k** means that motion in the transverse directions is completely neglected in the high-energy approximation.

Replacing the unperturbed Hamiltonian H_0 in the expression for the Green's function (2.2) by the eikonal Hamiltonian $\widetilde{H}_0$, we define an eikonal Green's function $\widetilde{g}_0$:

$$\widetilde{g}_0 = (E - \widetilde{H}_0 + io)^{-1}. \quad (2.9)$$

In momentum representation, the functions g_0 and $\widetilde{g}_0$ differ little from one another within a small solid angle around the direction of **k**. For sufficiently high energies of the incident particle, this angular region is of the greatest interest since the scattering amplitude at high energies is significantly different from zero in precisely that region (Fig. 1).

Using Eq. (2.8) for the eikonal Hamiltonian, it is easy to find an explicit expression for the function $\widetilde{g}_0$. In coordinate representation, the eikonal Green's function $\widetilde{g}_0$ has the form[19]

$$\widetilde{g}_0(\mathbf{r}, \mathbf{r}') = \int \frac{d\mathbf{p}}{(2\pi)^3} \frac{e^{i\mathbf{p}(\mathbf{r}'-\mathbf{r})}}{-\frac{1}{\mu}(\mathbf{p}-\mathbf{k})\mathbf{k} + io}$$
$$= -i\frac{\mu}{k}\delta(\boldsymbol{\rho}' - \boldsymbol{\rho})\,\theta(z'-z)\,e^{ik(z'-z)}, \quad (2.10)$$

where $\theta(x)$ is the Heaviside function

$$\theta(x) = \begin{cases} 1, & x > 0; \\ 0, & x < 0. \end{cases}$$

The presence of the delta function $\delta(\boldsymbol{\rho}' - \boldsymbol{\rho})$ in the eikonal Green's function $\widetilde{g}_0(\mathbf{r}, \mathbf{r}')$ ($\boldsymbol{\rho}$ and $\boldsymbol{\rho}'$ are radius vectors in the plane perpendicular to the vector **k**) is directly associated with the neglect of transverse motion of the particle.

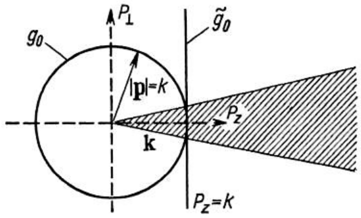

Fig. 1. Properties of the Green's functions g_0 and $\widetilde{g}_0$ in the momentum plane. The region in which the scattering amplitude is significantly different from zero is shaded.

If in the Hamiltonian (2.7) we take into account the change in the transverse component of the momentum (neglecting, as before, the change in the longitudinal component), the following expression can be obtained for the Green's function:

$$\widetilde{g}_0'(\mathbf{r}, \mathbf{r}') = -\frac{\mu}{2\pi}\cdot\frac{\theta(z'-z)}{(z'-z)}\,e^{ik\left\{z'-z+\frac{(\boldsymbol{\rho}'-\boldsymbol{\rho})^2}{2(z'-z)}\right\}}. \quad (2.11)$$

Note that Eq. (2.11) transforms into Eq. (2.10) when the condition $|z' - z| \ll k(\boldsymbol{\rho}' - \boldsymbol{\rho})^2$ is satisfied. The Green's function defined by Eq. (2.11), in contrast to that defined by Eq. (2.10), takes into consideration effects associated with deviation of particle motion from linear motion.

Substituting the function (2.10) in place of $g_0(\mathbf{r}, \mathbf{r}')$ in the Lippman–Schwinger equation (2.4), we obtain an ordinary differential equation of first order from the integral equation. It is easy to find a solution for this equation which also defines the wave function in the high-energy approximation:[20]

$$\psi_{\mathbf{k}}(\mathbf{r}) = e^{i\mathbf{kr} - i\frac{\mu}{k}\int_{-\infty}^{z} dz' V(\boldsymbol{\rho}, z')}. \quad (2.12)$$

It should be noted that Eq. (2.12) does not apply at too great a distance and therefore does not satisfy the boundary condition at infinity. Equation (2.12) can only be used when the condition $z < kr_0$ is satisfied.

Using the wave function (2.12), it is easy to find the scattering amplitude in the high-energy approximation. Substituting (2.12) into (2.6) and integrating by parts, we obtain for the scattering amplitude the well-known expression

$$f(\mathbf{k}, \mathbf{k}') = \frac{ik}{2\pi}\int d\boldsymbol{\rho}\, e^{i\mathbf{q}\boldsymbol{\rho}}\{1 - e^{2i\delta(\boldsymbol{\rho})}\}, \quad (2.13)$$

where $\mathbf{q} = \mathbf{k} - \mathbf{k}'$ is the change in momentum during scattering; $\delta(\boldsymbol{\rho})$ is the phase shift

$$2\delta(\boldsymbol{\rho}) = -\frac{\mu}{k}\int_{-\infty}^{\infty} dz V(\boldsymbol{\rho}, z). \quad (2.14)$$

Remember that the exact Green's function (2.5) was used in the derivation of Eq. (2.6) from (2.4).

In the high-energy approximation, one can obtain from the Lippman–Schwinger equation (2.4) another representation for the wave function which, in contrast to (2.12), is characterized by the proper asymptote. To do this, we pick out the z' component of the vector $\mathbf{r}'$ along the direction of **k** $[\mathbf{r}' \equiv \boldsymbol{\rho}' + (\mathbf{k}/k)z']$ and represent the function $g_0(\mathbf{r}, \mathbf{r}')$ in the form of a Fourier integral with respect to this component:

$$g_0(\mathbf{r}, \mathbf{r}') = \int_{-\infty}^{\infty} \frac{dk_z'}{2\pi} A_{k_z'}(\mathbf{r}, \boldsymbol{\rho}')\, e^{-ik_z' z'}. \quad (2.15)$$

For sufficiently large values of k ($kr_0 \gg 1$), the amplitude $A_{k'_z}$ is characterized by a sharp maximum for $k_z' = k$. Indeed, using Eq. (2.10) obtained in the high-energy approximation for the function $g_0(\mathbf{r}, \mathbf{r}')$, it is easy to show that the dependence on k_z' of the amplitude $A_{k'_z}(\mathbf{r}, \boldsymbol{\rho}')$ has the form of a delta function:

$$A_{k_z'}(\mathbf{r}, \boldsymbol{\rho}') \approx -\frac{2\pi i}{k}\mu\delta(\boldsymbol{\rho}' - \boldsymbol{\rho})\, e^{ikz}\delta(k_z' - k), \; z > kr_0^2.$$

Generally, the width of the maximum will be of the order of r_0^{-1}. Since the effective values of z' in $g_0(\mathbf{r}, \mathbf{r}')$ are of the order of magnitude of $\sim r_0$, the exponential in Eq. (2.15) changes slowly in the region of the maximum and its value for $k_z' = k$ can be taken outside the integral sign. The remaining integration gives the value of the function g_0 at the point $\mathbf{r}' = \boldsymbol{\rho}'$. In the high-energy approximation, therefore, the Green's function (2.15) can be approximated by

$$g_0(\mathbf{r}, \mathbf{r}') \approx e^{-ikz'} g_0(\mathbf{r}, \boldsymbol{\rho}'). \quad (2.16)$$

Substituting (2.16) in the Lippman–Schwinger equation (2.4) and using Eq. (2.12) for the wave function inside the integral sign, we obtain

$$\psi_{\mathbf{k}}(\mathbf{r}) = e^{i\mathbf{k}\mathbf{r}} - \frac{k}{2\pi i} \int d\boldsymbol{\rho}' \frac{e^{ik|\mathbf{r}-\boldsymbol{\rho}'|}}{|\mathbf{r}-\boldsymbol{\rho}'|} \{1 - e^{2i\delta(\boldsymbol{\rho}')}\} e^{i\mathbf{k}\boldsymbol{\rho}'}. \quad (2.17)$$

The integration in Eq. (2.17) is carried out over a plane perpendicular to the direction of the momentum of the incident particle ($\mathbf{k}\boldsymbol{\rho}' = 0$).

The wave function given by Eq. (2.17) has the correct asymptote, i.e., at infinity it is in the form of a sum of an incident plane wave and a diverging spherical wave for which the amplitude agrees with the previously determined expression (2.13) for the scattering amplitude. If Eq. (2.12) for the wave function is valid in the region of interaction (with respect to the variable z) $z < kr_0^2$, Eq. (2.17) is valid when the opposite condition, $z > kr_0^2$, is satisfied, i.e., outside the region of interaction. In contrast to Eq. (2.12), which depends directly on the potential $V(\mathbf{r})$, Eq. (2.17) is completely determined by a given scattering phase shift $\delta(\boldsymbol{\rho})$.

Equation (2.17) directly reflects the diffraction nature of high-energy scattering. Indeed, it was assumed in the derivation of Eq. (2.17) that small scattering angles are important [the main contribution to the integral is made by the region $z \gg k(\boldsymbol{\rho} - \boldsymbol{\rho}')^2$]; consequently

$$\frac{k}{2\pi i} \int d\boldsymbol{\rho}' \frac{e^{ik|\mathbf{r}-\boldsymbol{\rho}'|}}{|\mathbf{r}-\boldsymbol{\rho}'|} \approx e^{i\mathbf{k}\mathbf{r}}. \quad (2.18)$$

Using this relation, the wave function (2.17) is conveniently represented in the form

$$\psi_{\mathbf{k}}(\mathbf{r}) \approx \frac{k}{2\pi i} \int d\boldsymbol{\rho}' \frac{e^{ik|\mathbf{r}-\boldsymbol{\rho}'|}}{|\mathbf{r}-\boldsymbol{\rho}'|} e^{2i\delta(\boldsymbol{\rho}')} \varphi_{\mathbf{k}}(\boldsymbol{\rho}'), \quad (2.19)$$

where $\varphi_{\mathbf{k}}(\boldsymbol{\rho}') \equiv e^{i\mathbf{k}\boldsymbol{\rho}'} = 1$. Such a description of the wave function makes it possible to consider the scattering as diffraction and Eq. (2.19) can be interpreted as a generalized Huygens principle.[21] Indeed, the function $\varphi_{\mathbf{k}}(\mathbf{r}) = e^{i\mathbf{k}\boldsymbol{\rho}'}$ is an incident plane wave. In the plane of integration in Eq. (2.19), which passes through the center of the scattering field and is perpendicular to k, the amplitude of the incident wave at any point is unity, $\varphi_{\mathbf{k}}(\boldsymbol{\rho}') = 1$. The presence of a scattering field leads to the appearance of the phase factor $e^{2i\delta(\boldsymbol{\rho}')}$ inside the integral sign in Eq. (2.19), the phase shift $\delta(\boldsymbol{\rho}')$ of which depends on the distance at which the particle passes from the center of the scattering field. (In the high-energy approximation, it is assumed the particle moves on a linear trajectory.) If we set $e^{2i\delta}(\boldsymbol{\rho}') = 0$ for some region in the plane and $e^{2i\delta}(\boldsymbol{\rho}') = 1$ in the remainder, Eq. (2.19) transforms directly into the Kirchhoff formula which describes diffraction at an opaque screen.

In considering nuclear diffraction processes, it is convenient to represent the scattering amplitude (2.13) in the form

$$f(\mathbf{q}) = \frac{ik}{2\pi} \int d\boldsymbol{\rho} e^{i\mathbf{q}\boldsymbol{\rho}} \omega(\boldsymbol{\rho}), \quad (2.20)$$

where the so-called profile function

$$\omega(\boldsymbol{\rho}) \equiv 1 - e^{2i\delta(\boldsymbol{\rho})}. \quad (2.21)$$

is introduced in place of the phase shift $\delta(\boldsymbol{\rho})$. The profile function $\omega(\boldsymbol{\rho})$ defines the scattering amplitude in ρ representation. The quantities $f(\mathbf{q})$ and $\omega(\boldsymbol{\rho})$ are related through a two-dimensional Fourier transform;

$$\omega(\boldsymbol{\rho}) = \frac{1}{2\pi ik} \int d\mathbf{q} e^{-i\mathbf{q}\boldsymbol{\rho}} f(\mathbf{q}). \quad (2.22)$$

The function $\omega(\boldsymbol{\rho})$, like the phase shift $\delta(\boldsymbol{\rho})$, completely characterizes the scattering properties of a system. According to the definition (2.21), the profile function $\omega(\boldsymbol{\rho})$ is different from zero only for values of ρ less than the radius r_0 of the region of interaction. For $\rho > r_0$, the function $\omega(\boldsymbol{\rho})$ steeply falls to zero. We recall that the condition for applicability of the diffraction description reduces to the requirement

$$kr_0 \gg 1. \quad (2.23)$$

Setting r_0 equal to the range of nuclear forces, it is easy to see that the diffraction description will be valid for nucleon energies of the order of several hundred MeV and above.

3. DIFFRACTION NATURE OF NUCLEON INTERACTIONS AT HIGH ENERGIES

Experimental data on nucleon–nucleon scattering at high energies (of the order of several hundred MeV and above in the laboratory system) show that interactions between nucleons at high energies is of a diffraction nature. The angular distribution in elastic scattering is characterized by a sharp maximum in the forward direction, the width of which is determined by the range of nuclear forces. In addition to elastic scattering, inelastic scattering or nucleon absorption accompanied by pion formation occurs in this energy region. The total cross sections for elastic scattering and absorption are approximately equal and change slowly with energy.

The nature of the angular dependence for nucleon–nucleon elastic scattering at high energies is well represented by the choice of an elastic scattering amplitude in the form of a sum of Gaussian functions of the momentum transfer:

$$f(q) = \frac{k\sigma}{4\pi}(\gamma e^{-aq^2} + ie^{-bq^2}), \quad (3.1)$$

where k is the momentum of the incident nucleon; σ is the total nucleon–nucleon cross section; γ is the ratio between the real and imaginary parts of the scattering amplitude at zero angle. Values of the parameters a, b, γ, and σ are determined from experimental data. The values of these parameters are somewhat different for different charge states and change somewhat with energy.[1)] For example, in the case of proton–proton and proton–neutron scattering at E = 1000 MeV, these parameters are[24]

$$\sigma_{pp} = 47.5 \text{ mb}; \quad a_{pp} = b_{pp} = 0.109 \text{ F}^2;$$
$$\gamma_{pp} = -0.05; \quad \sigma_{pn} = 40.4 \text{ mb};$$
$$a_{pn} = b_{pn} = 0.109 \text{ F}^2; \quad \gamma_{pn} = -0.50. \tag{3.2}$$

At lower energies (of the order of several hundred MeV), it is necessary to take into account the differences in the angular dependences of the real and imaginary parts of the amplitude; it is also necessary to consider the spin part of the amplitude. Thus, at a proton energy of 185 MeV, the dependence of the scalar portion of the amplitude agrees with Eq. (3.1) for the following parameter values:[18]

$$\sigma_{pp} = 25 \text{ mb}; \quad a_{pp} = 0,471 \text{ F}^2; \quad b_{pp} = 0.264 \text{ F}^2;$$
$$\gamma_{pp} = 1.225;$$
$$\sigma_{pn} = 47.7 \text{ mb}; \quad a_{pn} = 0.486 \text{ F}^2; \quad b_{pn} = 0.348 \text{ F}^2;$$
$$\gamma_{pn} = 0.842. \tag{3.3}$$

At the present time, the amplitude (3.1) cannot be obtained theoretically because of the lack of a systematic theory for strongly interacting particles.

Diffraction phenomena also occur in the interaction of nucleons with nuclei. In nucleon scattering by medium and heavy nuclei, diffraction characteristics appear even at energies of the order of a few tens of MeV. At such energies, the mean free path of a nucleon in nuclear matter is less than nuclear dimensions; therefore the nucleus can be considered as an absorber with respect to the nucleon wave. Nuclear diffraction phenomena in this energy range can be considered analogous to the diffraction of light in the presence of an absorber having the shape and dimensions of the nucleus (see refs. 25-27). However, we shall not consider diffraction phenomena in this energy region in this review. As the energy of the incident nucleon increases, the mean free path in nuclear matter becomes longer. Thus, for nucleon energies of the order of hundreds of MeV and more, the nucleus becomes transparent to the incident particles, and the optical model of a black or semitransparent nucleus used to describe nucleon–nucleus scattering at low energy is inapplicable. Nevertheless, the angular dependence of nucleon–nucleus scattering even at such high energies is characterized by a series of diffraction maxima and minima. Diffraction structure in the angular distribution can be explained in terms of interference between single, double, etc., scattering of incident particles by individual nucleons in the nucleus.

4. SCATTERING BY A SYSTEM OF BOUND PARTICLES

We consider scattering of high-energy particles by a system consisting of N bound particles. Assuming that the kinetic energy of an incident particle is large in comparison with the binding energy of the individual particles, interactions of the incident particle with particles comprising the system can be considered independently. In the case of two-particle forces, the total scattering phase shift $\delta_{(N)}(\boldsymbol{\rho})$ can be represented in the form of a sum of scattering phase shifts for individual particles $\delta_i(\boldsymbol{\rho} - \boldsymbol{\rho}_i)$ in accordance with Eq. (2.14):

$$\delta_{(N)}(\boldsymbol{\rho}) = \sum_i \delta_i(\boldsymbol{\rho} - \boldsymbol{\rho}_i), \tag{4.1}$$

where $\boldsymbol{\rho}$ and $\boldsymbol{\rho}_i$ are plane vectors which correspond to the projections of the radius vector $\mathbf{r}$ of the incident particle and the radius vectors $\mathbf{r}_i$ of the scattering particles on a plane perpendicular to the direction of the initial momentum of the incident particle. If the wavelength of the incident particle is small in comparison with the characteristic radii of the regions of interaction for the individual particles, the diffraction approximation is applicable. We define the overall profile function for the system $\omega_{(N)}(\boldsymbol{\rho})$ as

$$\omega_{(N)}(\boldsymbol{\rho}) \equiv 1 - e^{2i\sum_i \delta_i(\boldsymbol{\rho} - \boldsymbol{\rho}_i)}. \tag{4.2}$$

Obviously, the overall profile function $\omega_{(N)}$ can be expressed through the profile functions ω_i characterizing scattering by individual particles:

$$\omega_{(N)}(\boldsymbol{\rho}) = 1 - \prod_{i=1}^{N} \{1 - \omega_i(\boldsymbol{\rho} - \boldsymbol{\rho}_i)\}. \tag{4.3}$$

The two-particle profile function ω_i is related to the two-particle amplitude by Eq. (2.22).

By considering the diffraction of a particle by the individual particles of a bound system, it is easy to determine the wave function for the entire system by means of the generalized Huygens principle. This wave function can be written as the product of a wave function describing the relative motion of the scattered particle and the system and a wave function describing the internal motion of the particles in the system. In the case of elastic scattering, where the internal state of the scattering system remains unchanged, the wave function for relative motion at large distances has the form of a sum of an incident plane wave and a diverging spherical wave. In the case of inelastic scattering, where the state of the system changes, the wave function for relative motion at large distances contains only the diverging spherical wave. Using the asymptotic form of the functions mentioned, the scattering amplitude for a particle scattered by a system of bound particles (nucleus) is easily obtained in the form[12]

$$F_{0f}(q) = \frac{ik}{2\pi} \int d\boldsymbol{\rho}\, e^{i\mathbf{q}\boldsymbol{\rho}} (\Phi_f, \omega_{(N)}(\boldsymbol{\rho})\Phi_0), \tag{4.4}$$

where $\mathbf{q} = \mathbf{k} - \mathbf{k}'$ is the change in the momentum of the incident particle during scattering ($\mathbf{k}$ and $\mathbf{k}'$ are the particle momenta before and after collision); Φ_0 and Φ_f are the internal wave functions of the scattering system before and after collision.

The total interaction cross section is determined by the imaginary part of the elastic scattering amplitude for zero angle:

$$\sigma_t = \frac{4\pi}{k} \operatorname{Im} F_{00}(0). \tag{4.5}$$

Using Eq. (4.4), we then obtain the following expression:

$$\sigma_t = 2\,\mathrm{Re}\int d\boldsymbol{\rho}\,(\Phi_0,\, \omega_{(N)}(\boldsymbol{\rho})\,\Phi_0). \quad (4.6)$$

The total cross section for the interaction of a particle with a complex system is not equal to the sum of the total cross sections for the interaction of a particle with the individual particles in the system. This is due to the existence of multiple-scattering effects which break down the additivity of the cross sections. Actually, the right side of Eq. (4.3) can be identically represented as the sum

$$\omega_{(N)} = \sum_i \omega_i - \sum_{i>j} \omega_i\omega_j + \sum_{i>j>k} \omega_i\omega_j\omega_k - \ldots + (-1)^{N-1}\,\omega_N\omega_{N-1}\ldots\omega_2\omega_1. \quad (4.7)$$

The physical significance of the individual terms on the right side is easily ascertained. The quantity ω_i defines the amplitude for scattering by an individual particle. Therefore the first term on the right side describes independent scattering by individual particles, the second term takes into account effects associated with double scattering, the third term is associated with triple scattering, etc.

We shall give an explicit expression for the elastic scattering amplitude under the assumption there are no correlation between particles in the complex system (nucleus). In this instance, the square of the modulus of the wave function is represented as a product of individual particle densities

$$|\Phi_0|^2 = \prod_{i=1}^{N} \rho(\mathbf{r}_i), \quad (4.8)$$

and the amplitude for elastic scattering by a complex system consisting of identical particles takes the form

$$F_{00}(q) = \frac{ik}{2\pi}\int d\boldsymbol{\rho}\, e^{i\mathbf{q}\boldsymbol{\rho}} \times \left\{1 - \left[1 - \frac{1}{2\pi ik}\int d\mathbf{q}'\, e^{-i\mathbf{q}'\boldsymbol{\rho}} f(\mathbf{q}')\, s(\mathbf{q}')\right]^N\right\}, \quad (4.9)$$

where $s(\mathbf{q})$ is a form factor associated with the single-nucleon density:

$$s(\mathbf{q}) = \int d\mathbf{r}\, e^{i\mathbf{q}\mathbf{r}} \rho(\mathbf{r}). \quad (4.10)$$

Using asymptotic wave functions, one can also obtain expressions for the integrated absorption and scattering cross sections. The integrated cross sections for elastic and inelastic scattering are given by the expression

$$\sigma_{0f} = \int d\boldsymbol{\rho}\, |(\Phi_f,\, \{1 - e^{2i\sum_{i=1}^{N}\delta(\boldsymbol{\rho}-\boldsymbol{\rho}_i)}\}\,\Phi_0)|^2. \quad (4.11)$$

Using the completeness of the wave functions, one can obtain the following expression for the total integrated scattering cross section:

$$\sigma_s \equiv \sum_f \sigma_{0f} = \int d\boldsymbol{\rho}\,(\Phi_0,\, |1 - e^{2i\sum_{i=1}^{N}\delta(\boldsymbol{\rho}-\boldsymbol{\rho}_i)}|^2\,\Phi_0). \quad (4.12)$$

This cross section describes processes for which the number of particles in the scattering system remains unchanged, namely: elastic scattering, scattering of a particle with excitation of the scattering system, and scattering accompanied by partial or complete dissociation of the scattering system.

The integrated cross section for various reactions induced by the incident particle is given by

$$\sigma_r = \int d\boldsymbol{\rho}\,(\Phi_0,\, \{1 - e^{-4\,\mathrm{Im}\sum_{i=1}^{N}\delta(\boldsymbol{\rho}-\boldsymbol{\rho}_i)}\}\,\Phi_0). \quad (4.13)$$

The reaction cross section describes all processes in which the number of particles in the scattering system changes, namely: absorption of the incident particle by the scattering system and capture by the incident particle of one or several particles from the scattering system.

The cross section for the capture reaction, in which the incident particle captures a nucleon from the scattering system (nucleus), is

$$\sigma_{(1)} = \int d\boldsymbol{\rho}\,(\Phi_0,\, \{1 - e^{-4\,\mathrm{Im}\,\delta(\boldsymbol{\rho}-\boldsymbol{\rho}_1)}\}\, e^{-4\,\mathrm{Im}\sum_{i=2}^{N}\delta(\boldsymbol{\rho}-\boldsymbol{\rho}_i)}\,\Phi_0), \quad (4.14)$$

Since $\mathrm{Im}\,\delta \geq 0$, the cross section $\sigma_{(1)}$ is always less than the total reaction cross section σ_r.

The results obtained are applicable not only to the scattering of a particle by a system of bound particles, but also to the scattering of a complex system of interacting particles by a scattering center (a particle remaining in an unchanged state). Equations (4.11) and (4.12) will describe elastic and inelastic scattering of a complex particle, and Eq. (4.13), the reaction cross section. In particular, Eq. (4.14) will determine the cross section for the stripping reaction, in which one of the particles initially a component of the incident system is captured by the scattering system.

5. DIFFRACTION SCATTERING OF HIGH-ENERGY NUCLEONS BY LIGHT NUCLEI

We consider in detail the scattering of a high-energy nucleon by the simplest nucleus: the deuteron. According to Eqs. (4.4) and (4.7), the scattering amplitude for elastic scattering of a nucleon by a deuteron can be represented as a sum of the scattering amplitudes for an incident nucleon scattered by a neutron and by a proton, multiplied by a form factor associated with the internal structure of the deuteron and an additional amplitude which takes into account simultaneous scattering of the incident nucleon by the neutron and proton:

$$F_{00}(q) = [f_n(\mathbf{q}) + f_p(\mathbf{q})]\, s\left(\frac{\mathbf{q}}{2}\right) + \frac{i}{2\pi k}\int d\mathbf{q}'\, f_n\left(\frac{\mathbf{q}}{2}+\mathbf{q}'\right) f_p\left(\frac{\mathbf{q}}{2}-\mathbf{q}'\right) s(\mathbf{q}'), \quad (5.1)$$

where

$$s(\mathbf{q}) = \int d\mathbf{r}\, e^{i\mathbf{q}\mathbf{r}} \varphi_0^2(\mathbf{r}) \quad (5.2)$$

and φ_0 is the wave function for the ground state of the deuteron. Using Eq. (5.1) and the optical relation (4.5), it is easy to obtain the following expression for the total cross section for interaction of a nucleon with a deuteron:

$$\sigma_t=\sigma_n+\sigma_p+\frac{2}{k^2}\,\mathrm{Re}\int d\mathbf{q} f_n(\mathbf{q}) f_p(-\mathbf{q})\, s(\mathbf{q}), \qquad (5.3)$$

where σ_n and σ_p are respectively the total cross sections for interaction of the incident particle with a free neutron or proton. If the amplitudes f_n and f_p are purely imaginary, the added term in the total cross section (5.3) associated with double scattering is negative. Assuming the dimensions of the deuteron are considerably greater than the radius of the region in which the incident particle interacts with individual nucleons in the deuteron, one can take the value of the amplitudes at the point $\mathbf{q} = 0$ outside the integral sign in Eq. (5.3) and thus obtain the Glauber approximation:[28]

$$\sigma_t=\sigma_n+\sigma_p-\frac{1}{4\pi}\left\langle\frac{1}{r^2}\right\rangle\sigma_n\sigma_p. \qquad (5.4)$$

On the basis of Eqs. (5.3) and (5.4), one ordinarily determines the cross section for interaction of particles with a neutron from experimental data on the interaction of high-energy particles with deuterons.

Using the representation (3.1) for the nucleon–nucleon amplitude and choosing the wave function for the ground state of the deuteron in the form of a Gaussian, the amplitude (5.1) is easily determined in explicit form.[29] Figure 2 shows the dependence on momentum transfer of the portions of the amplitude (5.1) associated with single and double scattering, assuming $f_n = f_p$ and $\gamma = 0$. When $\mathbf{q} = 0$, the part of the amplitude associated with double scattering is considerably less than that associated with single scattering. However, the amplitude for double scattering at large values of q is considerably greater than the single-scattering amplitude because of a slow decrease as q increases. In the case of purely imaginary amplitudes f_n and f_p, the parts of the amplitude (5.1) associated with single and double scattering have opposite signs; thus the amplitude (5.1) goes to zero because of interference at a certain value of momentum transfer ($q \approx 0.6$ GeV/c). Since the amplitudes f_n and f_p actually have a small real part, the cross section for deuteron scattering should not go to zero, but should have a clearly defined interference minimum. Figure 3 shows the angular dependence of the proton–deuteron scattering cross section at an energy E = 1000 MeV calculated from Eq. (5.1), together with an experimental angular dependence.[30] Calculated and experimental values of the cross section are in good agreement over a wide range of angles with the exception of the region of the interference minimum. This discrepancy is associated with the fact that asphericity of the deuteron resulting from the noncentral nature of the nuclear interaction plays an important role in the region of the interference minimum. The discrepancy can be completely explained by consideration of deuteron asphericity.[31] The value of the cross section in the region of the interference minimum is very sensitive to the D-wave weight in the ground state of the deuteron. It is therefore possible to determine the D-wave weight in the ground state of the deuteron with great accuracy ($p_D = 6.7\%$) from data on scattering of nucleons and pions by deuterons by having available reliable values for single-nucleon amplitudes.

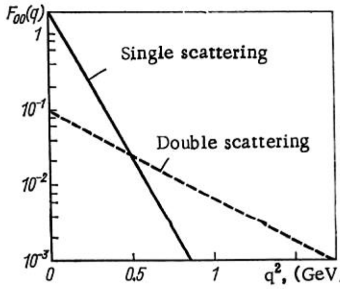

Fig. 2. Contribution of single and double scattering to the proton–deuteron elastic scattering amplitude.

We now turn to a consideration of scattering of high-energy nucleons by light nuclei. Neglecting correlation between nucleons in the nucleus and selecting a Gaussian for the single-nucleon density distribution, the nucleon–nucleus elastic scattering amplitude at high energy is easily found in explicit form:[14]

$$F_{00}(q)=f(0)\sum_{n=1}^{N}(-1)^{n-1}\frac{1}{n}\binom{N}{n}\left[\frac{\sigma(1-i\gamma)}{8\pi(a+\beta)}\right]^{n-1}e^{-\frac{a+\beta}{n}q^2}, \qquad (5.5)$$

$$s(q)=e^{-\beta q^2}.$$

The terms in Eq. (5.5) associated with higher powers, i.e., higher collision multiplicities, fall more slowly as q increases. Collisions of low multiplicity make the main contribution at small scattering angles and collisions of high multiplicity at large scattering angles. If the real part of the single-nucleon amplitude is neglected, the terms in Eq. (5.5) will alternate in sign. Therefore a diffraction structure should be observed in the angular dependence of the cross section as the result of interference between individual terms in Eq. (5.5), namely, a sharp maximum associated with single scattering occurs when $\mathbf{q} = 0$; the second minimum because of interference between double and triple scattering, etc.

On the basis of the diffraction theory that has been developed, it is possible to obtain information about nuclear structure from experimental data on elastic scattering of high-energy nucleons by nuclei if the scattering amplitude of the nucleon at the corresponding energy is known for scattering by a free nucleon. In a number of papers,

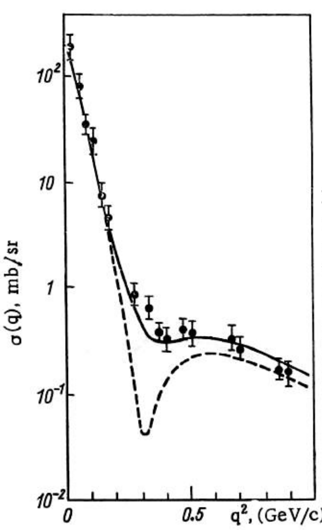

Fig. 3. Dependence of proton–deuteron elastic scattering differential cross section at 1000 MeV on q^2, momentum transfer squared;[15] dashed line) only S waves included in the deuteron ground state; solid line) admixture of D waves with a weight $p_D = 6.7\%$ included.

calculations have been made of the angular distributions for scattering of 1000-MeV protons by ^{4}He, ^{12}C, ^{16}O, and other nuclei.[24,32,33] The calculated results demonstrated the possibility for good agreement with experimental data.[34] This agreement made it possible to determine the real portions of single-nucleon amplitudes with great accuracy.[14,15] Figure 4 shows the differential cross section[24] for elastic scattering of 1000-MeV protons by ^{4}He. Curve 1 refers to consideration of single scattering only, curve 2 to consideration of single and double scattering, etc. From a comparison of calculated results and experimental data, it is possible to determine the size and shape of the nucleon and the nucleon density distribution in nuclei. Based on an analysis of experimental data for proton scattering, it was shown that the nucleon density distribution in nuclei was practically the same as the charge distribution.[35]

Cluster structure in the ^{6}Li nucleus was investigated in ref. 36 on the basis of diffraction analysis of data for elastic and inelastic scattering of 185-MeV protons by ^{6}Li. It was shown that it was impossible to explain the observed angular dependence for proton scattering within the framework of the simple shell model (as was also true for high-energy electron scattering[37]). Elastic scattering and inelastic scattering with excitation of the first 3^+ excited level (2.18 MeV) were considered. To describe the ^{6}Li states, cluster wave functions were used with parameters for d and α clusters corresponding to the values of the root-mean-square radii for free particles. The results of the calculations are shown[36] in Figs. 5 and 6. Good agreement with experimental data[38] can be achieved by selection of the value 0.45 for the cluster parameter x (ratio between the square of the α-particle radius).

The effect of deformation of the ^{12}C nucleus on elastic and inelastic (with nuclear transition to the first excited state) scattering of 1000-MeV protons was discussed in refs. 33 and 39. Single-particle wave func-

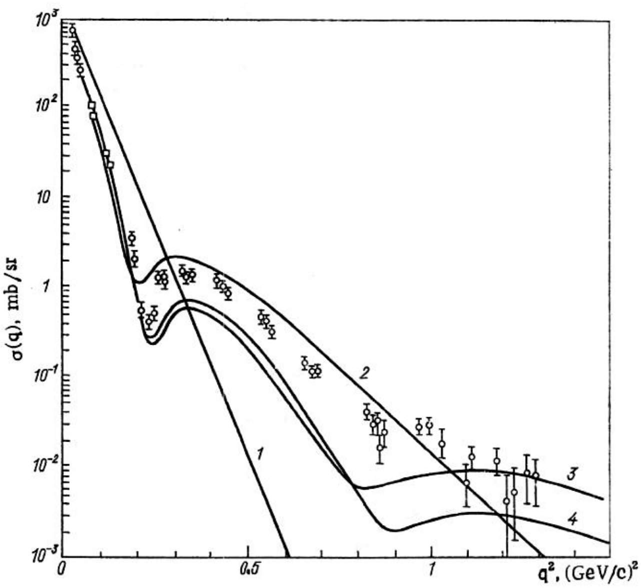

Fig. 4. Dependence of the differential cross section for elastic scattering of 1000-MeV protons by ^{4}He on q^2, momentum transfer squared;[24] 1) corresponds to single scattering alone (impulse approximation); 2) corresponds to single and double scattering, etc.

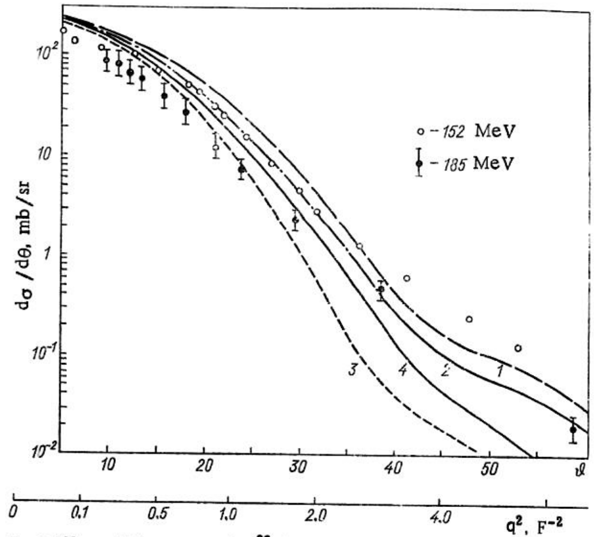

Fig. 5. Differential cross section[36] for elastic scattering of 185-MeV protons by ^{6}Li: 1) shell model; 2, 3, 4) cluster model of ^{6}Li for different parameter values.

tions for an anisotropic oscillator were used. Figures 7 and 8 show results of the calculations assuming small deformation.[33] The best agreement between the calculated angular distribution for elastically scattered protons and experimental data is achieved for a deformation parameter value $\beta = 1.35$. The value found for β was then used in calculation of the differential cross section for inelastic scattering. As a consequence, better agreement was obtained with experimental data than for the case of a spherically symmetric nucleus.

Information about nuclear structure can also be obtained by studying the integrated cross section (4.12) for inelastic nucleon–nucleus scattering. Since only a small portion of the energy is transferred to the nucleus in collisions of a high-energy nucleon with a nucleus, the completeness condition for the final nuclear states can be used in calculating the cross section. Consequently, the total inelastic scattering cross section will be determined only by the wave function for the ground state of the nucleus:

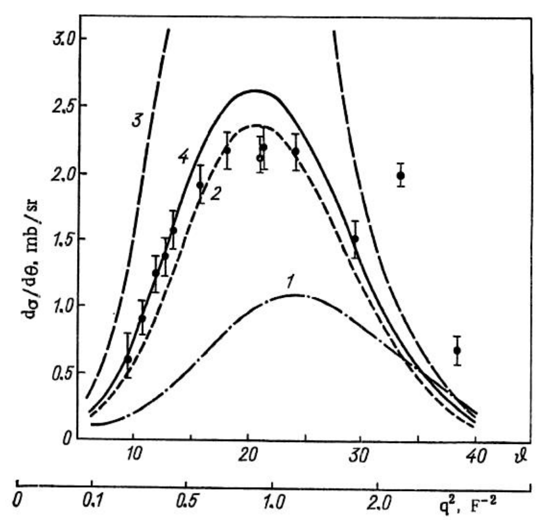

Fig. 6. Differential cross section[36] for inelastic scattering of 185-MeV protons by ^{6}Li with excitation of the 3^+ state (2.18 MeV); 1) shell model; 2, 3, 4) cluster model of ^{6}Li for different parameter values.

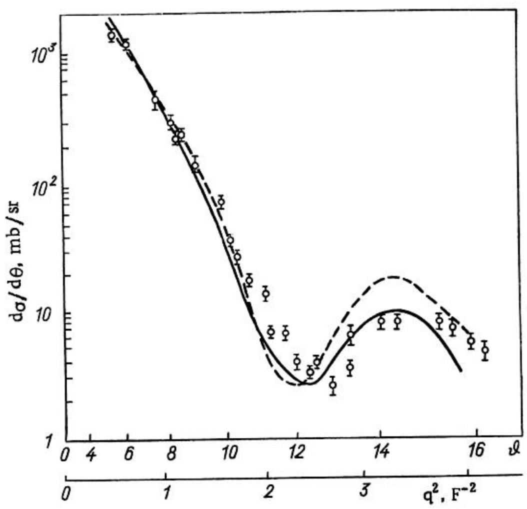

Fig. 7. Differential cross section for elastic scattering of 1000-MeV protons[33] by ^{12}C: dashed line) shell model; solid) including deformation of ^{12}C nucleus with a deformation parameter $\beta = 1.35$.

$$\sigma_{in}(q) = \sum_{f \neq 0} |F_{0f}(q)|^2. \tag{5.6}$$

Using Eq. (4.4), one can pick out the contributions from collision of different multiplicities in explicit form. Furthermore, regions in which some particular scattering multiplicity is predominant can be distinguished in the angular distribution. Comparison of calculated distributions with experimental distributions makes it possible to obtain data on density distribution in nuclei (nuclear radius, thickness of diffuse layer, absorption coefficient of nuclear matter, etc.). Figure 9 shows the cross section for inelastic scattering of protons by ^{12}C, calculated from the Glauber diffraction theory,[15] along with experimental data.

The examples given of the excellent agreement between calculations based on the diffraction concept for nucleon–nucleus interactions and experimental data are

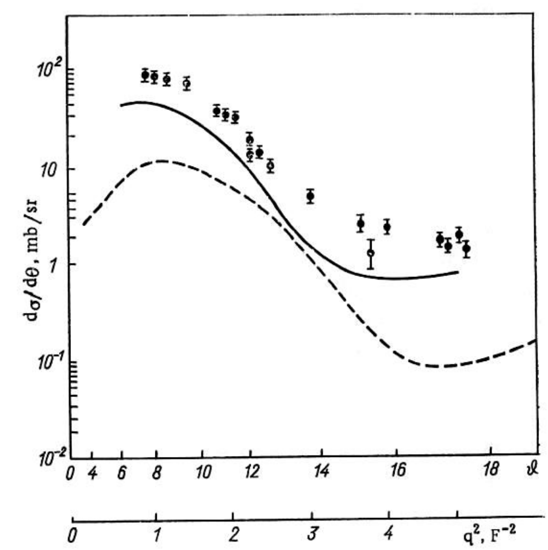

Fig. 8. Differential cross section for inelastic scattering of 1000-MeV protons by ^{12}C with excitation of the 2^+ state (4.44 MeV):[33] Dashed line) shell model; solid line) including nuclear deformation with deformation parameter $\beta = 1.35$.

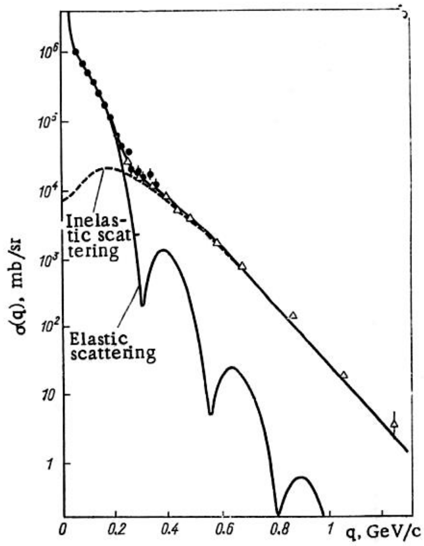

Fig. 9. Dependence of the integrated cross section for the scattering of approximately 20-GeV protons by ^{12}C on the momentum transfer q:[15] solid line) elastic scattering; dashed line) inelastic scattering.

evidence of the broad possibilities for using nuclear diffraction processes to study both nuclear structure and the nature of nucleon–nucleon interactions.

6. EFFECTS OF MULTIPLE SCATTERING AND THE IMPULSE APPROXIMATION

To describe the interaction of high-energy nucleons with nuclei, one also often uses the impulse approximation,[3] for which the region of applicability overlaps the region of applicability for the diffraction approximation.

It is of interest to make a comparison of the approximations mentioned and to explain the fundamental difference between them.[18]

In the diffraction approximation, the amplitude for nucleon scattering by a system of N bound particles is given by the general equation (4.4) in which the overall profile function $\omega_{(N)}(\boldsymbol{\rho})$ should be taken in the form (4.7). If multiple scattering effects are completely neglected, i.e., only the first summation remains on the right side of Eq. (4.7), we obtain the following expression for the amplitude:

$$F_{0f}(q) \approx \frac{ik}{2\pi} \int d\rho e^{iq\rho} \left(\Phi_f, \sum_i \omega_i(\rho - \rho_i) \Phi_0\right). \tag{6.1}$$

This amplitude corresponds to a plane-wave impulse approximation in which scattering by individual particles is considered independently; furthermore, the effect of all other particles on the scattering is completely neglected.

In a more refined version of the impulse approximation, inclusion of the effect of the other particles in consideration of scattering by an individual particle reduces to the introduction of distortion of the wave functions of the scattered particle. The scattering amplitude corresponding to the impulse approximation with inclusion of distortion of the wave functions of the scattered particle can be obtained from Eq. (4.4) in the following way. We write the profile function (4.3) in the form

$$\omega_{(N)} = \sum_i \omega_i \prod_{j=1}^{i-1} (1-\omega_j) = \omega_N \prod_{j=1}^{N-1} (1-\omega_j) + \omega_{N-1} \prod_{j=1}^{N-2} (1-\omega_j) + \omega_2(1-\omega_1) + \omega_1. \tag{6.2}$$

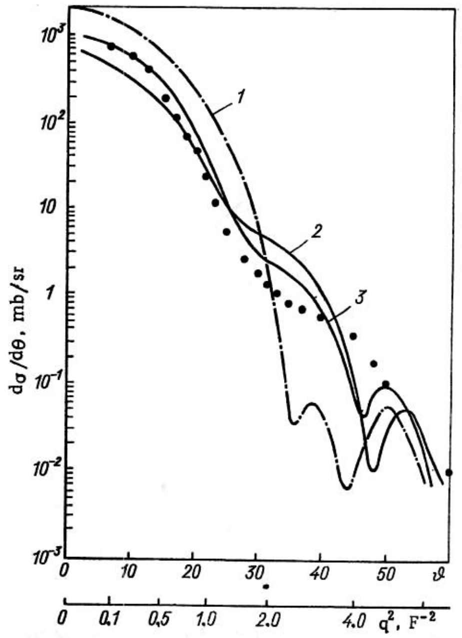

Fig. 10. Differential cross section for elastic scattering of 185-MeV protons by ^{12}C: 1) Plane-wave impulse approximation; 2) distorted-wave impulse approximation; 3) diffraction approximation.

tion equations are significantly different from the results obtained with the diffraction approximation. While the plane-wave impulse approximation overestimates the cross sections at small scattering angles, the distorted-wave impulse approximation underestimates the cross sections in the region of small angles. Where the diffraction approximation makes it possible to obtain the correct scattering cross sections at small angles without the introduction of any adjustable parameters, use of the impulse approximation leads to values greatly different in absolute magnitude. Note that the difference between the approximations mentioned is considerably greater at 1000 MeV.

7. INELASTIC NUCLEON SCATTERING WITH SMALL MOMENTUM TRANSFER

In considering inelastic nucleon–nucleus scattering accompanied by small momentum transfer, it is convenient to use the multipole expansion formalism.[10, 11] In accordance with Eqs. (6.1) and (2.22), the amplitude for the scattering of a particle by a system of bound particles can be written in the impulse approximation as

$$F_{0f}(q)=\left(\Phi_f,\ \sum_i e^{i\mathbf{q}\boldsymbol{\rho}_i} f_i(\mathbf{q})\,\Phi_0\right). \tag{7.1}$$

Since $\mathbf{q}$ is perpendicular to $\mathbf{k}$ under the conditions for applicability of the diffraction approximation, the plane vector $\boldsymbol{\rho}_i$ can be replaced by the vector $\mathbf{r}_i$ in the exponential inside the summation sign in Eq. (7.1). Assuming the scattering particles to be identical, it is convenient to relate the scattering amplitude (7.1) directly to the particle density operator $\hat{\rho}(\mathbf{r})=\sum_i \delta(\mathbf{r}-\mathbf{r}_i)$:

$$F(q)\equiv\sum_i e^{i\mathbf{q}\mathbf{r}_i} f_i(\mathbf{q})=f(q)\int d\mathbf{r}\, e^{i\mathbf{q}\mathbf{r}}\hat{\rho}(\mathbf{r}). \tag{7.2}$$

Expanding the plane wave inside the integral sign in Eq. (7.2) in spherical functions and introducing the density multipole moment of the system by means of the equality

$$\mathfrak{M}_{lm}(q)=\int d\mathbf{r}\, j_l(qr)\, Y_{lm}(\mathbf{n}_r)\,\hat{\rho}(\mathbf{r}), \tag{7.3}$$

it is easy to obtain the following multipole expansion for the scattering amplitude:

$$F_{0f}(q)=4\pi\sum_{lm} i^l Y^*_{lm}(\mathbf{n}_q)\, f(q)\,(\Phi_f,\ \mathfrak{M}_{lm}(q)\,\Phi_0). \tag{7.4}$$

Such a representation of the amplitude is convenient in considering transitions of the scattering system over a discrete spectrum because the individual multipoles in Eq. (7.4) are responsible for transitions under fixed selection rules.

In the general case, when considering spin and isospin degrees of freedom of interacting nucleons, one should choose a two-nucleon amplitude in the form

$$f_i=\sum_{tu}(-1)^u\,(A^t+\mathbf{B}^t\boldsymbol{\sigma}_i)\,\tau^{t-u}\tau_i^{tu},\quad t=0,\,1, \tag{7.5}$$

where $\boldsymbol{\sigma}$ and $\boldsymbol{\tau}$ are the spin and isospin matrices (τ^{tu} is the spherical tensor operator in isotopic spin space). If the amplitude (7.5) is given in the center-of-mass system of the two nucleons, it is necessary to include an additional factor μ'/μ in Eq. (7.4) where μ is the reduced mass of the two-nucleon system and μ' is the reduced mass of the nucleon–nucleus system. The complex coefficients A and B appearing in the amplitude (7.5) are matrices in spin space of the incident nucleon and depend on its energy and on the momentum transfer $\mathbf{q}$. Furthermore, in describing inelastic nuclear transitions, it is necessary to introduce[10] in addition to the density multipole moment (7.3) the longitudinal spin, electric, and magnetic multipole moments $\mathfrak{M}^L$, $\mathfrak{M}^E$, and $\mathfrak{M}^M$.

Multipole moments are described by irreducible tensor operators of rank l and t respectively in ordinary and charge space. For a given value of l, the density and electric multipole moments $\mathfrak{M}$ and $\mathfrak{M}^E$ are characterized by the parity $(-1)^l$; the longitudinal spin and magnetic multipole moments $\mathfrak{M}^L$ and $\mathfrak{M}^M$ are characterized by the opposite parity $(-1)^{l+1}$. The parity value is directly related to the sign of the multipole operator transformation for spatial reflection.

We shall characterize an initial state by assignment of the quantum numbers J for the spin, M for the spin projection, T for the isospin, and N for the isospin projection of the nucleus, μ and ν for the spin projection and isospin projection of the scattered nucleon; the corresponding values after scattering will be indicated by primes.

Using the Wigner–Eckart theorem, it is easy to pick out an explicit dependence on magnetic quantum numbers in the matrix elements of the multipole moment operators. Introducing the abbreviated notation for reduced matrix elements of the multipole operators

$$I_{lt}(q)\equiv\sqrt{\frac{4\pi}{(2J'+1)(2T'+1)}}\,\langle J'T'\,\|\,\mathfrak{M}_l^t\,\|\,JT\rangle, \tag{7.6}$$

we finally obtain the following expression for the multipole expansion of the scattering amplitude:

We consider scattering by the last, or N-th, particle and account for the effect of all other particles [first term in the sum in Eq. (6.2)] on the assumption that there are no correlations between the particles in the scattering system. We consider a single-particle transition in the system, associated with a change in the state of the N-th particle, and we shall assume the state of the remaining particles is unchanged. In this case, the effect of the remaining particles on the scattering will be characterized by a factor in the amplitude which can be written as

$$\left(\Phi_0, \prod_{j=1}^{N-1} (1-\omega_j)\Phi_0\right) = \left(1 - \frac{1}{2\pi ik}\int d\mathbf{q}' e^{i\mathbf{q}'\boldsymbol{\varrho}} f(\mathbf{q}')\, s(\mathbf{q}')\right)^{N-1} \quad (6.3)$$

when one takes into account identity of the particles and normalization of single-particle wave functions. Assuming $N \gg 1$, the right side of Eq. (6.3) can be represented by an exponential

$$\left(\Phi_0, \prod_{j=1}^{N-1} (1-\omega_j)\Phi_0\right) \approx e^{2i\delta(\boldsymbol{\varrho})};\ 2\delta(\boldsymbol{\rho}) = -\frac{\mu}{k}\int_{-\infty}^{\infty} dz \mathscr{V}(\boldsymbol{\rho}, z), \quad (6.4)$$

where $\mathscr{V}(\boldsymbol{\rho}, z)$ is the optical potential

$$\mathscr{V}(\boldsymbol{\rho}, z) = -\frac{N}{4\pi^2\mu}\int d\mathbf{q}' e^{i\mathbf{q}'\mathbf{r}} f(\mathbf{q}')\, s(\mathbf{q}') \quad (6.5)$$

(μ is the reduced mass of the scattered and scattering particles).

If it is assumed that the subsequent terms in Eq. (6.2) make the same contribution to the scattering amplitude as the first term, then

$$F_{0f}(q) \approx \frac{ik}{2\pi}\int d\boldsymbol{\rho}\, e^{i\mathbf{q}\boldsymbol{\varrho}+2i\delta(\boldsymbol{\varrho})}\left(\Phi_f, \sum_i \omega_i(\boldsymbol{\rho}-\boldsymbol{\rho}_i)\Phi_0\right). \quad (6.6)$$

In accuracy, this expression corresponds to the scattering amplitude in the distorted-wave impulse approximation. Actually, in the high-energy approximation, one can show that

$$e^{i\mathbf{q}\boldsymbol{\varrho}+2i\delta(\boldsymbol{\varrho})} \approx \psi^{*}_{\mathbf{k}'}(\mathbf{r})\,\psi_{\mathbf{k}}(\mathbf{r}), \quad (6.7)$$

where $\psi_{\mathbf{k}}(\mathbf{r})$ is the wave function for a particle with a given momentum $\mathbf{k}$ scattered in the field of the optical potential created by all the particles of the scattering system with the exception of the selected particle.

Derivation of Eq. (6.6) was based on the assumption all terms in Eq. (6.2) make an identical contribution to the amplitude. In fact, the structure of individual terms in Eq. (6.2) depends essentially on the number i of the selected particle. Therefore, Eq. (6.6), like Eq. (6.1), is an insufficiently exact expression for the scattering amplitude (4.4). We shall find a more exact expression for the scattering amplitude which logically takes account of the effects of multiple scattering in single-particle transitions. For this purpose, we write the profile function ω_N in a form which is symmetrized with respect to all the scattering particles:

$$\omega_{(N)} = \sum_i \omega_i \left\{1 - \frac{1}{2!}\sum_{j\neq i}\omega_j + \frac{1}{3!}\sum_{j\neq k\neq i}\omega_j\omega_k - \ldots + \frac{(-1)^{N-1}}{N!}\sum_{j\neq k\neq\ldots\neq i}\omega_j\omega_k\ldots\omega_n\right\}. \quad (6.8)$$

The individual terms in Eq. (6.8) can be reduced to one another by simple relabelling. If i = N, one can easily confirm by a direct check that the expression in braces in Eq. (6.8) can be written in the form $\int_0^1 dx \prod_{j=1}^{N-1}(1-x\omega_j)$.
We therefore have in the general case

$$\omega_{(N)} = \sum_i \omega_i \int_0^1 dx \prod_{j=1}^{N-1}(1-x\omega_j). \quad (6.9)$$

Neglecting correlations between scattering particles and assuming $N \gg 1$, we obtain

$$\left(\Phi_0, \int_0^1 dx \prod_{j=1}^{N-1}(1-x\omega_j)\Phi_0\right) \approx e^{i\delta(\boldsymbol{\varrho})}\frac{\sin\delta(\boldsymbol{\rho})}{\delta(\boldsymbol{\rho})}. \quad (6.10)$$

Thus, the scattering amplitude (4.4) can be represented approximately as

$$F_{0f}(q) \approx \frac{ik}{2\pi}\int d\boldsymbol{\rho}\, e^{i\mathbf{q}\boldsymbol{\varrho}+i\delta(\boldsymbol{\varrho})}\frac{\sin\delta(\boldsymbol{\rho})}{\delta(\boldsymbol{\rho})}\left(\Phi_f, \sum_i \omega_i(\boldsymbol{\rho}-\boldsymbol{\rho}_i)\Phi_0\right). \quad (6.11)$$

In contrast to the impulse approximation [Eqs. (6.1) and (6.6)], Eq. (6.11) logically takes into account the effect of multiple scattering during single-particle transitions.

As an illustration of the application of the approach developed, and for the purpose of a quantitative evaluation of the effects of multiple scattering, we consider the elastic scattering of 185- and 1000-MeV protons by the ^{12}C nucleus, for which there are experimental data. In calculation of the differential scattering cross section, we use Eq. (6.1) in the plane-wave impulse approximation, Eq. (6.6) in the distorted-wave impulse approximation, and Eq. (6.11) in the diffraction approximation.

We choose the nucleon–nucleon amplitude in the form (3.1) and the values of the parameters are respectively those in (3.2) and (3.3). To describe the ^{12}C ground state, we use an oscillator shell function with an oscillator parameter $\alpha = 0.609\ F^{-1}$.

The calculated results for the energies 185 and 1000 MeV are shown in Figs. 10 and 11, respectively. The curves 1 represent the differential scattering cross section calculated in the plane-wave impulse approximation on the basis of Eq. (6.1); the curves 2 show the differential scattering cross section calculated in the distorted-wave impulse approximation based on Eq. (6.6), and curves 3 show the differential scattering cross section calculated in the diffraction approximation based on Eq. (6.11). Figure 11 also shows (curve 4) the differential scattering cross section calculated on the basis of the exact diffraction-approximation equation (4.4). The plotted points represent experimental data taken from refs. 40 and 34.

As is clear from the figures, calculations based on the diffraction approximation are in best agreement with the experimental data. [Results of calculations based on the approximate diffraction equation (6.11) and the exact diffraction equation (4.4) are practically the same.] Calculated cross sections based on the impulse approxima-

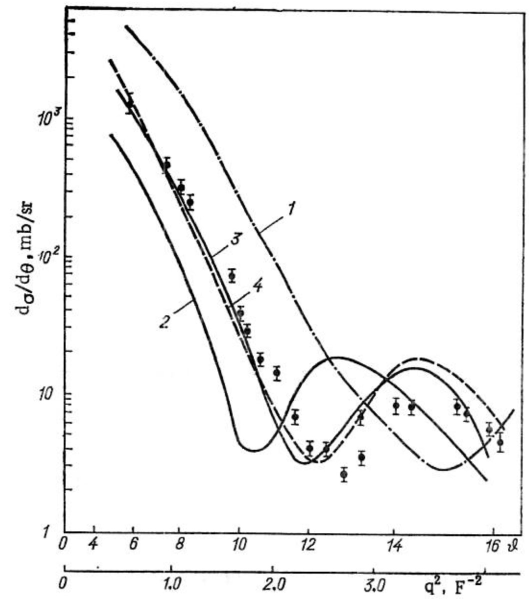

Fig. 11. Differential cross section for elastic scattering of 1000-MeV protons by ^{12}C: 1) Plane-wave impulse approximation; 2) distorted-wave impulse approximation; 3) simplified diffraction approximation (6.11); 4) diffraction approximation.

$$F_{0f}(q)=(-1)^{\nu-\nu'}\frac{\mu'}{\mu}\sum_{t}\sum_{lm} i^l\sqrt{(2l+1)(2t+1)}$$
$$\times(JMlm\,|\,J'M')\,(TNt\nu-\nu'\,|\,T'N')\left(\tfrac{1}{2}\nu t\nu'-\nu\,\middle|\,\tfrac{1}{2}\nu'\right)$$
$$\times\left\{[A^t_{\mu'\mu}I_{lt}(q)+B^t_{0,\,\mu'\mu}I^L_{lt}(q)]\,D^{l*}_{0m}(\mathbf{n}_q)\right.$$
$$\left.+\frac{1}{\sqrt{2}}\sum_{\lambda=\pm1}B^t_{-\lambda,\,\mu'\mu}[\lambda I^E_{lt}(q)+I^M_{lt}(q)]\,D^{l*}_{\lambda m}(\mathbf{n}_q)\right\}. \quad (7.7)$$

Averaging the square of the modulus of the transition amplitude (7.7) over the initial spin states of the scattered nucleon and the nucleus and summing over the final spin states, one can obtain the following expression for the nucleon–nucleus scattering cross section:

$$d\sigma=\frac{2J'+1}{2J+1}\left(\frac{\mu'}{\mu}\right)^2\frac{k'}{k}\sum_{tt'}\sum_{l}\eta_\nu\,(TNt0\,|\,T'N)\,(TNt'0\,|\,T'N)$$
$$\times\{P_{tt'}I_{lt}I^*_{lt'}+Q_{tt'}I^L_{lt}I^{L*}_{lt'}+R_{tt'}[I^E_{lt}I^{E*}_{lt'}+I^M_{lt}I^{M*}_{lt'}]\}\,do, \quad (7.8)$$

where we have used the notation

$$\eta_\nu=\begin{cases}1 & \nu={}^1/_2;\\(-1)^{t+t'}, & \nu=-{}^1/_2;\end{cases}$$

$$\left.\begin{aligned}P_{tt'}&=\frac{1}{2}\mathrm{Tr}A^tA^{t'\dagger};\quad Q_{tt'}=\frac{1}{2}\mathrm{Tr}B^t_0B^{t'\dagger}_0;\\R_{tt'}&=\frac{1}{2}\mathrm{Tr}B^t_{\pm1}B^{t'\dagger}_{\pm1}\end{aligned}\right\}. \quad (7.9)$$

The coefficients P, Q, and R are determined by the two-nucleon interaction and depend on the energy of the incident nucleon and the magnitude of the momentum transfer. All information about nuclear structure which is obtained through the study of nucleon–nucleus scattering is contained in the reduced matrix elements of the multipole moments.

It is immediately clear from the form of Eq. (7.7) that for specific nuclear transitions, we have the following selection rules for angular momentum, parity, and isospin:

$$|J'-J|\leqslant l\leqslant J'+J;\quad \pi\pi_l=\pi';\quad |T'-T|\leqslant t\leqslant T'+T;$$
$$N+\nu=N'+\nu', \quad (7.10)$$

where π and π' are the parities of the initial and final nuclear states and π_l is the parity of the multipole. The last equation is an expression of electric charge conservation in scattering.

According to Eq. (7.8), there is no interference between transitions of different nature or of different multipolarity. For fixed values of spin and isospin in the initial (J and T) and final (J' and T') states, the sums in Eq. (7.8) contain a finite number of terms in accordance with the selection rules (7.10).

For small values of q, transitions with lowest multipolarity are most probable. As q increases, transitions of higher multipolarities begin to appear. If $qR \approx 1$, where R is the nuclear radius, additive cross sections with different values of l become of the same order of magnitude.

In the case of elastic nucleon–nucleus scattering, the spin, isotopic spin and parity of the nucleus are unchanged ($J' = J$, $T' = T$, and $\pi' = \pi$). From parity conservation and reciprocity, it follows that a contribution to elastic scattering can only be made by even density multipoles and odd longitudinal spin and magnetic multipoles. Using Eq. (7.8), it is easy to obtain a general expression for the proton–nucleus elastic scattering cross section. For a spinless nucleus ($J = J' = 0$), only density monopole transitions are possible because of the rule for combination of moments. Therefore the cross section for elastic scattering by a spinless nucleus is given by

$$d\sigma=\left(\frac{\mu'}{\mu}\right)^2\left\{P_{00}\,|\,I_{00}\,|^2+\frac{N^2}{T(T+1)}P_{11}\,|\,I_{01}\,|^2\right.$$
$$\left.+\frac{2N}{\sqrt{T(T+1)}}\,\mathrm{Re}\,P_{01}I_{00}I^*_{01}\right\}do. \quad (7.11)$$

The form factors I_{00} and I_{01} are directly expressed through the nucleon density distribution and the isotopic charge for the nucleus in the ground state and have a diffraction structure with minima and maxima. In the limiting case of small momentum transfer ($q \to 0$), the quantities I_{00} and I_{01} reduce to the nucleon number A of the nucleus and to twice the value of the total isotopic spin of the nucleus:

$$I_{00}(q)=A\left(1-\frac{1}{6}q^2\langle r^2\rangle\right)\cdot$$
$$I_{01}(q)=2\sqrt{T(T+1)}\left(1-\frac{1}{6}q^2\langle r^2\rangle_1\right), \quad (7.12)$$

where $\langle r^2\rangle$ and $\langle r^2\rangle_1$ are respectively the mean-square radii of the nucleon density distribution and isotopic charge distribution in the ground state of the nucleus.

Knowing the quantities $P_{tt'}$, which are determined by the nature of the two-nucleon interaction, one can obtain from data on nucleon–nucleus elastic scattering direct information about nucleon and isotopic charge distribution in nuclei. If the isotopic spin of the nucleus in the ground state is zero, the nucleon–nucleus elastic scattering cross section depends only on the nucleon density distribution:

$$d\sigma = \left(\frac{\mu'}{\mu}\right)^2 P_{00} |I_{00}|^2 \, do. \qquad (7.13)$$

According to Eq. (7.12), the nucleon–nucleus scattering cross section in the region of small angles can be many times larger than the cross section for scattering by an individual nucleon.

In the case of nucleon scattering by nuclei with nonzero spin, not only does the density monopole interaction appear, but also density interactions of higher multipolarity and longitudinal spin and magnetic interactions. In elastic scattering, the spin and parity of the nucleus are unchanged; according to the selection rules, therefore, only even density multipole transitions $0 \leq l \leq 2J$ and odd longitudinal spin and magnetic multipole transitions $1 \leq l \leq 2J$ are possible.

For density transitions, the addition because of quadrupole interactions appears only when $J \geq 1$. In the limiting case of small momentum transfer, the quantity $I_{20}(q)$ is proportional to the value of the density quadrupole moment of the nucleus Q^A. The contribution of the quadrupole interaction to the scattering cross section is most important in the region of the minimum of $I_{00}(q)$.

If $J = 1/2$, addition to the density monopole transition is only possible because of longitudinal spin and magnetic dipole transitions. In the limiting case of small momentum transfer, the quantities $I_{10}^{L}(q)$ and $I_{10}^{M}(q)$ are expressed in terms of the value of the nuclear angular momentum which is associated with nucleon spins. The relative contribution of the density, longitudinal spin, and magnetic interaction to scattering at a given angle depends on the angular dependence of the coefficients P, Q, and R. Figures 12 and 13 show the angular dependence for the coefficients P, Q, and R at a nucleon energy of 185 MeV calculated from the experimental data.

If $J \geq 3/2$, longitudinal spin and magnetic moments of higher multipolarity will make a contribution to the scattering cross section. In the region of the minimum of $I_{10}^{L}(q)$, the octupole longitudinal spin moment $I_{30}^{L}(q)$ may make a noticeable contribution to the longitudinal spin portion of the cross section; similarly, the octupole magnetic moment $I_{30}^{M}(q)$ will appear in the region of the minimum of $I_{10}^{M}(q)$. The use of oriented nuclei and polarized nucleons makes it possible to obtain additional information about the properties of the ground state of the nucleus.

The cross section for inelastic nucleon–nucleus scattering, which is accompanied by a nuclear transition from the initial state to some excited state with an energy in

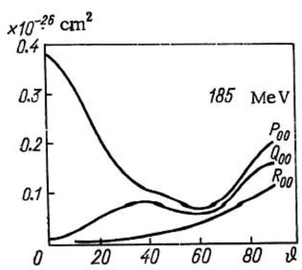

Fig. 12. Angular dependence of the scalar proton P, vector longitudinal proton P, and transverse R of the nucleon–nucleon interaction for transitions without isospin change.

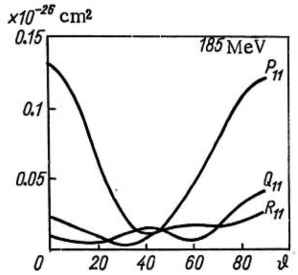

Fig. 13. Angular dependence of the scalar proton P, vector longitudinal portion Q, and transverse portion R of the nucleon–nucleon interaction for transitions with a change in isospin.

the region of the discrete spectrum, is defined by the general equation (7.8). Multipoles with $t = 0$ are responsible for transitions in which the isotopic spin of the nucleus is unchanged ($\Delta T = 0$). Multipoles with $t = 1$ are responsible for transitions in which the isotopic spin of the nucleus is either unchanged [$\Delta T = 0$, but the nuclear isospin must be nonzero ($T \neq 0$)] or changes by unity ($\Delta T = \pm 1$).

In the case of small momentum transfer, we have $\mathfrak{M}_l^t \sim q^l$ for an arbitrary density multipole. Therefore, knowing the dependence of the form factor on q, one can determine the multipolarity of a transition and consequently the spin of the initial or final state of the nucleus. If the relative parity of the initial and final states of the nucleus agrees with $(-1)^{J-J'}$, the multipole with $l = |J - J'|$ makes the greatest contribution to scattering; furthermore, the angular dependence is determined by the matrix element

$$I_{lt} \sim q^{|J-J'|}. \qquad (7.14)$$

In particular, if $J' = J$, the main contribution is made by the monopole. Since for small momentum transfer

$$\mathfrak{M}_{00}^{00}(q) = \frac{1}{\sqrt{4\pi}} \left\{ A - \frac{q^2}{6} \int dr\, r^2 \hat{\rho}^{00}(r) + \ldots \right\} \qquad (7.15)$$

and the second term of the expansion in Eq. (7.15) is responsible for the inelastic transition, angular dependence will be determined by the matrix element

$$I_{0t} \sim q^2.$$

Note that a quadrupole transition also leads to the same sort of angular dependence.

If the relative parity of the initial and final states of the nucleus is opposite to $(-1)^{|J-J'|}$, the multipole with $l = |J - J'| + 1$ makes the largest contribution to scattering and the angular dependence is determined by the matrix element

$$I_{lt} \sim q^{|J-J'|+1}. \qquad (7.16)$$

Note that for density multipole transitions, the inelastic scattering cross section goes to zero when $\mathbf{q} = 0$.

For electric multipole transitions, we have the selection rules

$$|J - J'| \leqslant l \leqslant J + J', \quad l \geqslant 1, \quad \Delta\pi = (-1)^l.$$

If the relative parity of the initial and final states agrees with $(-1)^{J-J'}$, the largest contribution to scattering for small q is made by the multipole with $l = |J - J'|$ for the case $J \neq J'$ and by the multipole with $l = 2$ for $J = J'$.

For longitudinal spin and magnetic transitions, we have the selection rules

$$|J-J'|\leqslant l\leqslant J+J',\ l\geqslant 0 \text{ for } L,\ l\geqslant 1 \text{ for } M,$$
$$\Delta\pi=(-1)^{l+1}.$$

If the relative parity of the initial and final states of the nucleus agrees with $(-1)^{J-J'}$, the main contribution to scattering is made by multipoles with $l = |J - J'| + 1$ and the angular dependence is determined by the matrix element

$$I_{lt}^{L,M}\sim q^{|J-J'|}. \tag{7.17}$$

If $J = J' \neq 0$, $I_{lt}^{L,M} \sim 1$; in this case, the scattering cross section is nonzero even when $q = 0$. If the relative parity of the initial and final states of the nucleus is opposite to $(-1)^{J-J'}$, the main contribution is made by multipoles with $l = |J - J'|$ and the angular dependence is determined by the matrix element

$$I_{lt}^{L,M}\sim q^{|J-J'|-1},\quad J\neq J'. \tag{7.18}$$

When $J = J'$, we assume the values $l = 0$ for I_{lt}^{L} and $l = 2$ for I_{lt}^{M} with

$$I_{0t}^{L},\ I_{2t}^{M}\sim q.$$

Experimental data on the excitation of levels in light nuclei by 185-MeV protons[38,41] agree with the rules specified.

If the nuclear spin in the initial state is zero ($J = 0$), only transitions with the multipolarity $l = J'$ are possible. For a relative parity of initial and final states which agrees with $(-1)^{J'}$, only density and electric transitions are allowed (longitudinal spin and magnetic transitions are forbidden). For relative parity of the initial and final states which is opposite to $(-1)^{J'}$, on the other hand, longitudinal spin and magnetic transitions are allowed (density and electric transitions are forbidden). If $J' = 0$ also, only the density monopole transition $0^+ \to 0^+$ and the longitudinal spin transition $0^+ \to 0^-$ are allowed.

To calculate the reduced matrix elements of multipole operators, it is necessary to know the nuclear wave functions. At the present time, such calculations can be performed for different nuclear models. Furthermore, it turns out that the nature of the angular distribution and absolute value of a cross section is very sensitive to the choice of model. Therefore a comparison of calculated and experimental values can be an important source for determining the nature of nuclear states.

As in the plane-wave case, it is also convenient to expand in multipole moments when considering transitions in a system including the multipole scattering amplitude (6.11). Expressing the scattering amplitude (6.11) through the density operator $\hat{\rho}(\mathbf{r})$, we obtain

$$F(q)=\frac{ik}{2\pi}\int d\mathbf{r}'\left[\int d\mathbf{x}e^{i\mathbf{q}\mathbf{x}+i\Phi(\rho'+x)}\omega(\mathbf{x})\right]e^{i\mathbf{q}\mathbf{r}'}\hat{\rho}(\mathbf{r}'); \tag{7.19}$$

$$\Phi(\rho)=\delta(\rho)-i\ln\frac{\sin\delta(\rho)}{\delta(\rho)} \tag{7.20}$$

(a new variable of integration $\mathbf{x} = \boldsymbol{\rho} - \boldsymbol{\rho}'$ is introduced in place of $\boldsymbol{\rho}$). In the integration on the right side of Eq. (7.19), effective values of x will be of the same order of magnitude as the range r_0 of the forces between the particles while the effective values of r' will be of the order of the dimension R of the scattering system. If $r_0 \ll R$, the effective values of x will be considerably less than the effective values of r'. Since the phase function $\Phi(\boldsymbol{\rho})$ is a smooth function of its argument, it can be expanded in a series in powers of x and consideration limited to the linear term. In this case, the variables in the right side of Eq. (7.19) are separable and we have as a result

$$F(q)=f(\tilde{q})\int d\mathbf{r}e^{i\mathbf{q}\mathbf{r}+i\Phi(\rho)}\hat{\rho}(\mathbf{r}), \tag{7.21}$$

where $\tilde{\mathbf{q}}$ is the effective value of the momentum transfer:

$$\tilde{\mathbf{q}}\approx\mathbf{q}+\nabla_\rho\Phi(\rho)|_{\rho\approx R}.$$

Note that the difference between the effective value of the momentum transfer $\tilde{\mathbf{q}}$ and $\mathbf{q}$ is connected with consideration of the finite range of the forces. Replacement in Eq. (7.21) of the effective value $\tilde{\mathbf{q}}$ by $\mathbf{q}$ corresponds to the assumption of zero range for the forces.

Using Eq. (7.21), it is not difficult to represent the transition amplitude including multiple scattering effects (6.11) in a form similar to Eq. (7.4) if the multipole moment is defined by the equality

$$\tilde{\mathfrak{M}}_{lm}(q)=\int d\mathbf{r}\varphi_{lm}(r)Y_{lm}(\mathbf{n}_r)\hat{\rho}(\mathbf{r}), \tag{7.22}$$

where the function $\varphi_{lm}(r)$ is related to the phase function $\Phi(\boldsymbol{\rho})$ by

$$\varphi_{lm}(r)=\sum_{l'l''}(-1)^{(l-l'+m)/2}\frac{(2l'+1)(2l''+1)}{(2l+1)}\frac{\sqrt{(l''-m)!(l''+m)!}}{(l''-m)!!(l''+m)!!}$$
$$\times(l'ol''o|lo)(l'ol''m|lm)j_{l'}(qr)\Phi_{l''}(r); \tag{7.23}$$

$$\Phi_l(r)=(-1)^{l/2}\int_0^1 dxP_l(x)e^{i\Phi(r\sqrt{1-x^2})}. \tag{7.24}$$

[In the distorted-wave impulse approximation, the multipole moment is also given by Eq. (7.22); in this case, one should set $\Phi = 2\delta$.]

The selection rules for parity and angular momentum for scattering with inclusion of multiple-scattering effects remain the same as for the plane-wave approximation. Inclusion of multiple scattering leads to a significant change in the radial dependence of the multiple moments, namely, to a replacement of the spherical Bessel functions $j_l(qr)$ by the complex functions $\varphi_{lm}(\mathbf{r})$, which lead to an additional dependence on m in the reduced matrix elements.

As an example of the use of the multipole formalism, we consider inelastic scattering of high-energy protons by the carbon nucleus ^{12}C. The ground state of ^{12}C is characterized by the quantum numbers $J = 0$, $\pi = 1$, and $T = 0$. As in the case of elastic scattering, we shall use the shell model with an oscillator potential for description of the ^{12}C nucleus.

We use the distorted-wave impulse approximation.

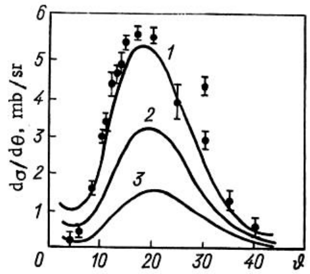

Fig. 14. Angular dependence of the cross section for inelastic scattering of 185-MeV protons by ^{12}C with excitation of the 2^+, T = (4.4 MeV) state: 1) Random-phase model; 2) Tamm–Dancoff model; 3) independent-particle model.

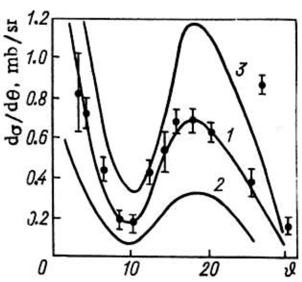

Fig. 15. Angular dependence of the cross section for inelastic scattering of 185-MeV protons by ^{12}C with excitation of the 0^+, T = 0 (7.65 MeV) state; 1) wave function (7.25); 2) Tamm–Dancoff model; 3) independent-particle model.

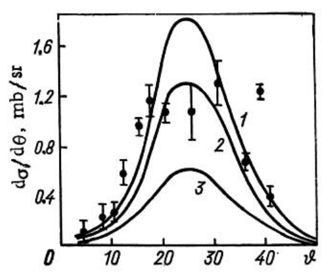

Fig. 16. Angular dependence of the cross section for inelastic scattering of 185-MeV protons by ^{12}C with excitation of the 3^-, T = 0 (9.64 MeV) state: 1) Random-phase mode ; 2) Tamm–Dancoff model; 3) independent-particle model.

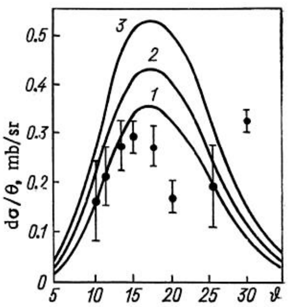

Fig. 17. Angular dependence of the cross section for inelastic scattering of 185-MeV protons by ^{12}C with excitation of the 2^+, T = 1 (16.11 MeV) state: 1) random-phase model; 2) Tamm–Dancoff model; 3) independent-particle model.

The optical potential, which describes refraction and absorption of the nucleon wave within the nucleus, can be determined by considering that refraction and absorption are caused by multiple scattering processes which occur because of interactions of the wave with individual nucleons in the nucleus. In this case, the optical potential is expressed in terms of the scattering amplitude for nucleon–nucleon scattering and the nucleon density distribution in the nucleus. For a nucleus in which J = T = 0 in the ground state, the contribution to the optical potential is made by the scalar portion of the two-nucleon scattering amplitude, which is independent of the spin and isospin operators of the nuclear nucleon.

Figures 14-17 give the calculated results for the inelastic scattering cross section of 185-MeV protons scattered by the ^{12}C nucleus with the excitation of the following states:

$$2^+T=0\ (4.44\ \text{MeV});\qquad 0^+T=0\ (7.65\ \text{MeV});$$
$$3^-T=0\ (9.64\ \text{MeV})\ \text{and}\ 2^+T=1\ (16.11\ \text{MeV}).$$

Curves 1 and 2 in these figures correspond to the shell model with residual interaction: 1 corresponds to the random-phase model (except for the 0^+ state) and 2 to the Tamm–Dancoff model; curve 3 corresponds to the independent-particle model. Curve 1 for the 0^+ state corresponds to the following wave function:

$$|0^+T=0\rangle = -0.321\,|2s_{1/2}1s_{1/2}^{-1}\rangle + 0.947\,|2p_{3/2}1p_{3/2}^{-1}\rangle, \quad (7.25)$$

which was obtained from matching of the calculated and experimental cross sections. A more detailed description of the models used is given in ref. 10. The figures make it clear that the nature of the angular dependence of the differential cross sections and their absolute values are in good agreement with the experimental values.[41] Calculation of the cross sections for inelastic transitions with excitation of the states 1^+, T = 0 (12.71 MeV) and 1^+, T = 1 (15.11 MeV) also leads to the correct angular dependence; however, the absolute values of the cross sections are approximately four times greater than the experimental values.[11] As a rule, the shell model with residual interaction (random-phase model) gives better agreement with experiment than other models of the nucleus, which is in accordance with calculated results for the cross sections for inelastic scattering of fast electrons by nuclei.[42]

The multipole formalism was also used in a discussion of the scattering of fast pions by nuclei.[43]

* * *

The examples discussed show that elastic and inelastic scattering of high-energy nucleons by nuclei are well described on the basis of a diffraction approach taking into account the effects of multiple scattering. A satisfactory explanation of numerous experiments in which high-energy interactions not only of nucleons, but also of pions and other strongly interacting particles were studied was obtained within the framework of diffraction theory. Establishment of the diffraction nature of nuclear interactions at high energies makes it possible to use these processes for the study of nuclear structure. Consideration of the diffraction nature of high-energy interactions also makes it possible to obtain information about the hadron–nucleon interaction from data on the interaction of high-energy hadrons with nuclei. Interesting possibilities for using high-energy hadrons to study nuclear structure and the nature of nuclear interactions are discussed in ref. 44.

1) The dependence of amplitude on momentum transfer in the form of Gaussians was first proposed by Belen'kii in the analysis of pion–proton scattering[22] and by Grishin and Saitov in the analysis of proton–proton scattering.[23]

1T. De Forest and J. Walecka, Adv. Phys., 15, 1 (1966).
2A. G. Sitenko, Lectures at Third All-Union School on Nuclear Physics,

Khumann, 1967 (Nuclear Structure [in Russian], Izd. AN UkrSSR, Tashkent (1969), p. 91).
[3]A. K. Kerman, H. McManus, and R. M. Thaler, Ann. Phys., 8, 551 (1959).
[4]Y. Nishida, Nucl. Phys., 43, 598 (1963).
[5]R. M. Haybron and H. McManus, Phys. Rev., 136B, 1730 (1964); 140B, 638 (1965).
[6]R. M. Haybron, M. B. Johnson, and R. J. Metzger, Phys. Rev., 156, 1136 (1967).
[7]H. K. Lee and H. McManus, Phys. Rev., 161, 1087 (1967).
[8]R. M. Haybron, Nucl. Phys., A124, 662 (1969).
[9]B. P. Bannik, V. L. Lyuboshits, and M. N. Podgoretskii, JINR Preprint R-2881, Dubna (1966).
[10]A. G. Sitenko, I. S. Dotsenko, and A. D. Firsa, Ukr. Fiz. Zh., 16, 555 (1971).
[11]A. G. Sitenko, A. D. Fursa, and I. S. Dotsenko, Ukr. Fiz. Zh., 16, 881 (1971).
[12]A. G. Sitenko, Ukr. Fiz. Zh., 4, 152 (1959).
[13]R. Glauber, Lectures in Theoretical Physics, W. Brittin and L. Dunham, eds., Interscience, New York (1959), p. 315.
[14]R. Glauber, High-Energy Physics and Nuclear Structure, G. Alexander (ed.), North-Holland, Amsterdam (1967), p. 311.
[15]R. Glauber, High-Energy Physics and Nuclear Structure, S. Devons (ed.), Plenum Press, New York (1970), p. 207.
[16]A. G. Sitenko, Vest. AN UkrSSR, 12, 9 (1971)
[17]A. G. Sitenko, Lectures at Fourth All-Union School on Nuclear Physics, Kiev (1968) [Lecture Texts, Izd. Kiev University (1968)].
[18]A. G. Sitenko and I. S. Dotsenko, Yad. Fiz., 17, 67 (1973) [Sov. J. Nucl. Phys., 17, (1973) (in press)].
[19]T. A. Osborn, Ann. Phys. (N. Y.), 58, 417 (1970).
[20]L. D. Landau and E. M. Lifshitz, Quantum Mechanics, Addison–Wesley (1958)].
[21]A. G. Sitenko and V. V. Peresypkin, Teor. Matem. Fiz., 13 (1972).
[22]S. Belen'kii, Zh. Eksp. Teor. Fiz., 30, 983 (1956); 33, 1248 (1957) [Sov. Phys.–JETP, 3, 813 (1956); 6, 960 (1958)].
[23]V. Grishin and I. Saitov, Zh. Eksp. Teor. Fiz., 33, 1051 (1957) [Sov. Phys.–JETP, 6, 809 (1958)].
[24]R. Bessel and C. Wilkin, Phys. Rev., 174, 1179 (1968).
[25]A. I. Akhiezer and I. Ya. Pomeranchuk, Usp. Fiz. Nauk, 39, 153 (1949).
[26]A. I. Akhiezer and A. G. Sitenko, Ukr. Fiz. Zh., 3, 16 (1958).
[27]I. S. Shapiro, Usp. Fiz. Nauk, 75, 61 (1961) [Sov. Phys.–Usp., 4, 674 (1962)].
[28]R. Glauber, Phys. Rev., 100, 242 (1955).
[29]A. G. Sitenko, Zh. Eksp. Teor. Fiz., 36, 1419 (1959) [Sov. Phys.–JETP, 9, 555 (1959)].
[30]G. Bennet et al., Phys. Rev. Lett., 19, 387 (1967).
[31]V. Franco and R. Glauber, Phys. Rev. Lett., 22, 370 (1968).
[32]W. Czyz and L. Lesniak, Phys. Rev. Lett., 24B, 227 (1967).
[33]I. S. Dotsenko and A. D. Fursa, Yad. Fiz., 17 (1973) [Sov. J. Nucl. Phys., 17 (1973) (in press)].
[34]H. Palevsk et al., Phys. Rev. Lett., 18, 1200 (1967).
[35]R. Glauber and G. Matthiae, Nucl. Phys., B21, 135 (1970).
[36]I. S. Dotsenko and A. D. Fursa, Yad. Fiz., 17 (1973) [Sov. J. Nucl. Phys., 17 (1973) (in press)].
[37]Yu. A. Kudeyarov et al., Nucl. Phys., A163, 316 (1971).
[38]R. M. Hutcheon, O. Sundberg, and G. Tibell, Nucl. Phys., A154, 261 (1970).
[39]H. Lesniak and L. Lesniak, Nucl. Phys., B25, 525 (1971).
[40]A. Johansson, V. Svanberg, and P. E. Hodgson, Arkiv for Fysik, 19, 541 (1961).
[41]D. Hasselgren et al., Nucl. Phys., 69, 81 (1965).
[42]V. Gillet and M. A. Melkanoff, Phys. Rev., 133B, 1190 (1964).
[43]A. G. Sitenko, I. S. Dotsenko, and A. D. Fursa, Ukr. Fiz. Zh., 16, 1676 (1971).
[44]W. Czyz, High-Energy Scattering from Nuclei, Preprint 697/PL/PH, Cracow (1970).